

Scanning electron microscope with polarization analysis: Micromagnetic structures in ultrathin films

Hans Peter Oepen^{a)}

*Institute of Applied Physics and Microstructure Advanced Research Center, University of Hamburg,
Jungiusstraße 11, D-20355 Hamburg, Germany*

Gerold Steierl and Jürgen Kirschner

Max Planck Institute of Microstructure Physics, Weinberg 2, D-0620 Halle, Germany

(Received 15 May 2002; accepted 16 September 2002)

The basics of the scanning electron microscope with polarization analysis are presented and special features of the microscope are discussed. The spin polarization of the secondary electrons allows for a high contrast as the topography of the sample is strongly suppressed. The feature of the method is that the orientation of the magnetization is measured and used for domain imaging. For complex domain patterns that makes the interpretation easy and direct. Examples are shown how the high surface sensitivity is used for the investigation of all kind of samples. The decoration by a thin ferromagnetic film makes even contaminated and samples with strongly spoiled surfaces accessible for scanning electron microscope with polarization analysis (SEMPA) investigation. Recently, the magnetic resolution of SEMPA has been pushed into the range of a few nm. © 2002 American Vacuum Society. [DOI: 10.1116/1.1519863]

I. INTRODUCTION

Scanning electron microscopy with polarization analysis (SEMPA) has developed into a powerful technique for the study of magnetic domains at surfaces and in ultrathin films. Many open questions concerning micromagnetic structures of mostly ideal systems have been answered utilizing SEMPA, e.g., the behavior of domain walls at the surface of bulk ferromagnets,^{1,2} the domain structure in ultrathin films,^{3,4} the spin reorientation in ultrathin films,^{5,6} and the exchange coupling in multilayers.⁷

II. BASICS

The technique utilizes the spin polarization of secondary electrons (SEs) created at the surface of itinerant ferromagnets to image the magnetic microstructure. At very low kinetic energies in the energy range of the intensity maximum of the secondary electrons an enhancement of the spin polarization is found.^{8,9} Based on this very favorable condition a microscope to image magnetic domains was proposed,^{10,11} and finally in 1984 the first SEMPA was realized.¹² The basic idea is to use the narrow primary beam of a scanning electron microscope (SEM) to create secondary electrons and analyze their spin polarization. Thus, the microscope is a SEM with an attached spin polarization analyzer. A sketch of the microscope is shown in Fig. 1. For the spin polarization analysis the electrons are scattered at a target. Different types of analyzers are used in SEMPA, like the Mott detector,^{13,14} the low energy diffuse scattering detector,¹⁵ or the low energy electron diffraction detector.¹⁶ In all analyzers the scattering into opposite angles is measured and compared. The intensity difference, normalized to the total scattering intensity, is proportional to the polarization component that is

perpendicular to the scattering plane. The normalization eliminates nearly all topographical structures in the polarization images allowing for higher magnetic contrast.¹³ Due to the extremely small depth of information of the spin polarization of the secondary electrons¹⁷ the experiment has to be performed under ultrahigh vacuum conditions. In principle the diameter of the primary beam determines the spatial resolution of the technique, provided that the beam current is high enough. As the efficiency of the spin-polarization analyzers are low (about 10^{-4}) in general, primary currents in the range of nA are needed to achieve images with good quality in reasonable times. To obtain the desirable high spatial resolution and high current electron sources with high brilliance, i.e., field emission sources are used in the microscope. Based on such a gun a SEMPA with a magnetic resolution of 5 nm has been realized recently.¹⁸ In a sophisticated design of such a microscope the complete detector attachment is optimized for utilizing almost all secondaries emitted within a certain energy window.¹⁹ In particular the acceptance angle has to be maximized, which is achieved by a geometry in which the electron optics (in front of the spin-polarization analyzer) is very close and perpendicular to the sample. Additionally, a high acceleration voltage is applied to the first elements of the optics in order to bend the secondary electrons toward the symmetry axis of the optics.

III. IMAGE FORMATION

In the early investigations of the spin polarized secondary electron (SE) emission it was found that the polarization vector is directly related to the magnetization orientation at the point of SE emission.²⁰ This finding is essential for SEMPA and represents the feature of the technique. Basically, the polarization direction is used to create the domain images. The vector of polarization can be obtained as two perpendicular polarization components are accessible in the scatter-

^{a)}Electronic mail: oepen@physnet.uni-hamburg.de

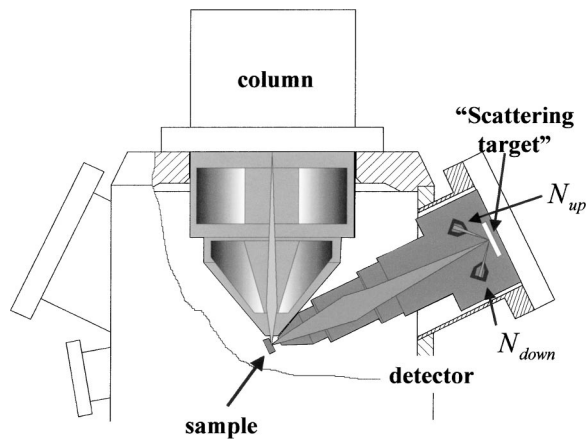


FIG. 1. Sketch of SEMPA. The primary beam from a SEM column creates secondary electrons that are collected and focused into the spin polarization analyzer. The secondary electrons are scattered at the target of the spin polarization detector. The scattering energy and material is different for the different types of analyzers used in SEMPA. In general, the scattering intensities in opposite angles are compared. The normalized intensity difference $(N_{up} - N_{down}) / (N_{up} + N_{down})$ is proportional to the polarization component perpendicular to the plane of drawing.

ing experiment that is utilized for the polarization analysis. An example of soft magnetic thin film structures is given in Fig. 2.²¹ The images display the spatial distribution of two polarization components and the topography image, measured simultaneously. The topography results as a byproduct of the spin analysis as the sum of all scattering intensities, and is from exactly the same sample area. The two polarization components can be put together by vectorial superposition, which yields the distribution of the magnetization orientation, i.e., the “complete” domain structure. A demonstration of a domain pattern showing the vector orientation of the magnetization is shown in Fig. 3. The image gives the complex domain pattern in a thin film soft magnetic disk. The color wheel in the lower part of the figure allows for the translation of the colors into the magnetization orientation within the film plane. The domain pattern is determined by magnetostatic energies which are dominant and a flux closure structure is observed. The structure represents a local energy minimum. The competing structure represent-

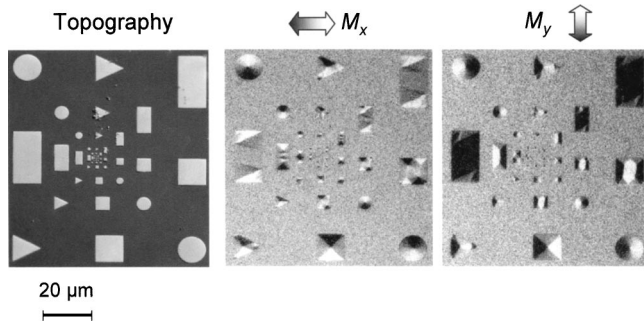


FIG. 2. Topography and domain pattern in Permalloy microstructures (see Ref. 24). The domain images show the magnetization distribution obtained in the two perpendicular polarization components. All three images were taken simultaneously. The Permalloy structures are 50 nm thick and deposited on oxidized Si.

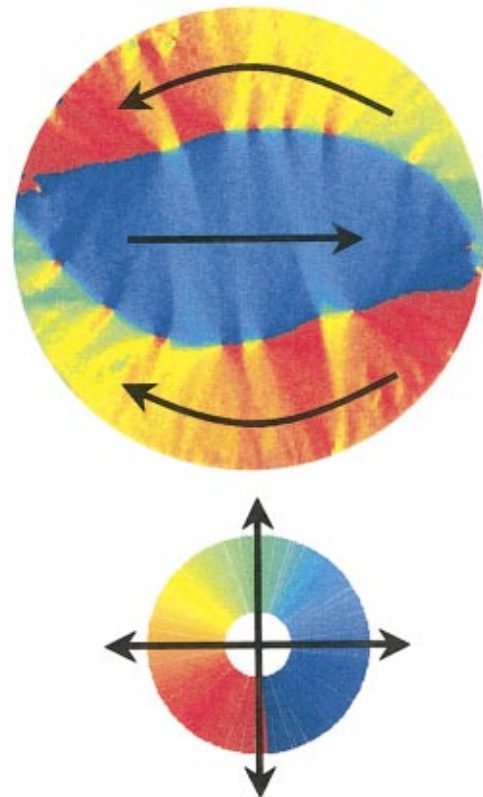


FIG. 3. Domain structure in a disk with a diameter of 10 μm (Ref. 21). The thickness of the polycrystalline Co disk is 50 nm. The colors represent different orientations of magnetization according to the color wheel given in the lower part. The arrows in the disk give the main orientation of magnetization. Domain walls are cross-tie walls.

ing the absolute minimum of energy is a vortex configuration that can be seen for example in Fig. 2 in the Permalloy thin film disks. The domain walls are cross-tie walls which can be recognized by the Néel-type legs that extend, perpendicular to the wall, throughout nearly the whole disk. A detail of the cross-tie wall is shown in the zoom in Fig. 4. To stress the point once more, the arrows plotted in the image (Fig. 4 left-hand side) are actually measured and not good guesses. A sketch of the cross-tie wall is shown on the right-hand side (Fig. 4).^{22,23} The vector plot clearly reveals all the details of the proposed model, particularly the two types of Bloch lines and the Néel-type legs.

IV. SAMPLE PREPARATION

SEMPA is known for its high surface sensitivity that is very favorable when ultrathin ferromagnets are in the focus of interest.¹⁹ For ideal systems, e.g., ultrathin epitaxial films, the surface sensitivity has been successfully demonstrated. In many discussions, however, this feature is quoted as a problem as it limits the applicability of SEMPA. Apparently, it restricts the application of SEMPA to systems with surfaces that are absolutely free from any contamination. In particular, systems that have been structured by lithography or other methods using multiple step preparation under ambient con-

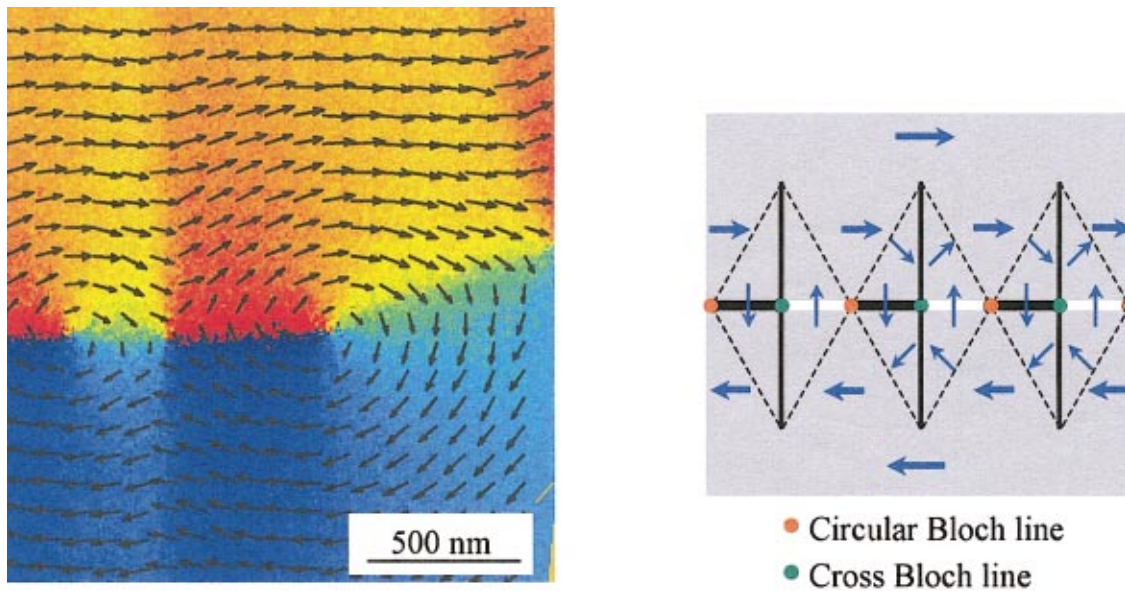


FIG. 4. Cross-tie wall in a thin film disk (see Refs. 21–24). The image is a zoom into the image shown in Fig. 3. On the right-hand side a sketch of the wall is displayed (see Ref. 27).

ditions seem to be inaccessible by SEMPA. The conditioning of such samples for SEMPA investigations has been studied recently.²⁴

For bulk as well as thick film samples surface preparation by simple ion milling is sufficient to allow for nearly perfect SEMPA investigation. This method has been successfully applied by different groups in many SEMPA studies. An example for the preparation of a film by ion milling is the structured magnetic film shown in Fig. 2, discussed above. The magnetic material was covered by a Cu layer prior to structuring to prevent spoiling of the surface. Before the SEMPA study the Cu layer was removed by ion milling. The magnetic patterns in the microstructures are the well known flux closure structures (Landau–Lifshitz structures) that have to be expected for Permalloy structures of such dimensions. The general finding is that the surface damage due to sputtering has no effect on the domain structure as long as the typical length of the magnetic structures is large compared to the depth of damage. In stable systems, like bulk ferromagnets, annealing by modest heating is possible which reduces the surface damage. In thin films, however, heating has to be prevented as it usually destroys the film composition. No remarkable effect on the polarization value (e.g., reduction) due to ion milling has been found.¹⁶

An even simpler and very effective method to prepare a sample for SEMPA investigation is to evaporate *in situ* a thin ferromagnetic film (Fe or Co) on top of the contaminated sample. It has been found that the thin film mirrors the domain structure of the ferromagnet beneath while the newly generated surface is clean and thus the SE are spin polarized. This so-called decoration technique has been successfully applied to different magnetic systems,²⁴ and has been already proposed in the early years of SEMPA investigations.²⁵ The images of the bars (Fig. 5) have been obtained by applying the decoration technique.

The bars have been covered by a Fe film of 10 monolayer thickness. The topography (left-hand side Fig. 5) is still dominated by remains of the photoresist that charge up. The magnetic microstructure in the central images, displaying the magnetization component along the long edges of the bars, reveals the domain structure. The bars with a flat end exhibit a flux closure structure at the ends while the pointed bars are single domain without any domain structure. Similar domain structures have been found for that kind of material and sample shape²⁶ which demonstrates that the domain structure in the bars determines the magnetic structure in the film. The decoration technique works although a contamination layer

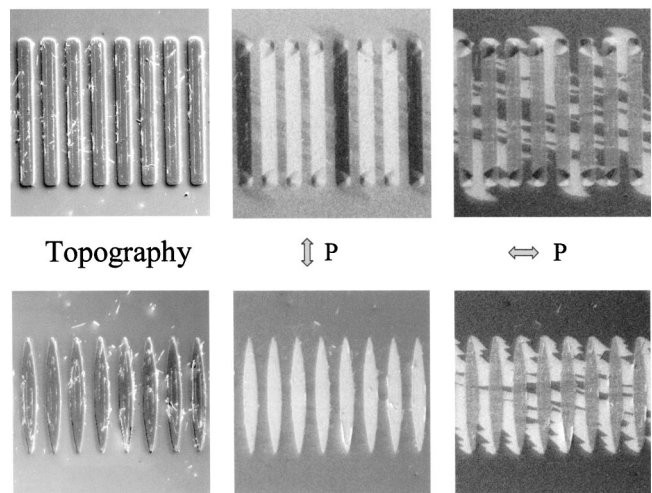


FIG. 5. Domain pattern in microstructures covered by a thin Fe film (see Ref. 21). The bars have a width of $2.5 \mu\text{m}$. The flat ended bars show a flux closure structure at the end, while bars with pointed ends are single domain. Note the domain structure in the film between the bars which is determined by the stray fields leaking out of the magnetic microstructures.

of unknown thickness separates the two ferromagnetic materials.

The magnetic structure in the second polarization component exhibits only black/white contrast outside the bars, which demonstrates that the film has uniaxial anisotropy. This domain pattern is due to the stray field generated by the bars. The competition between the stray field and the magnetic anisotropy of the film is responsible for the structure obtained. The decoration technique works as long as the magnetic material of the sample is thicker than the postdeposited film. Due to the high surface sensitivity of SEMPA, films with a thickness of a few monolayers are accessible utilizing this preparation technique.

The decoration technique may also be used to enhance the contrast. In low contrast materials a thin Fe film increases the spin polarization as Fe has the highest signal that can be achieved in SEMPA. Another advantage of the decoration technique is that nonitinerant and insulating ferromagnets can also be investigated by SEMPA. The decoration technique is superior to ion milling as effects like ion induced intermixing can be prevented. Last but not least the decoration technique makes the quality of the surface less important and the investigation of nearly all kinds of samples like, e.g., devices for commercial applications becomes feasible.

V. CONCLUSION

In summary, the improvement of SEMPA is still in the focus of basic research. The success of the technique is closely connected to developments at different frontiers of actual research. Spatial resolution in the range of 5 nm has been realized and the field of applicability has been expanded to nearly all kinds of samples.

ACKNOWLEDGMENT

The support from the "Bundesministerium für Bildung und Forschung" (Grant No. 13N7331/4) is gratefully acknowledged.

- ¹H. P. Oepen and J. Kirschner, Phys. Rev. Lett. **62**, 819 (1989).
- ²M. R. Scheinfein, J. Unguris, R. C. Celotta, and D. T. Pierce, Phys. Rev. Lett. **63**, 668 (1989).
- ³J. L. Robins, R. J. Celotta, J. Unguris, D. T. Pierce, B. T. Jonker, and G. A. Prinz, Appl. Phys. Lett. **52**, 1918 (1988).
- ⁴H. P. Oepen, J. Magn. Magn. Mater. **93**, 116 (1991).
- ⁵R. Allenspach, M. Stampanoni, and A. Bischof, Phys. Rev. Lett. **65**, 3344 (1990); R. Allenspach and A. Bischof, *ibid.* **69**, 3385 (1992).
- ⁶M. Speckmann, H. P. Oepen, and H. Ibach, Phys. Rev. Lett. **75**, 2035 (1995); H. P. Oepen, M. Speckmann, Y. T. Millev, and J. Kirschner, Phys. Rev. B **55**, 2752 (1997).
- ⁷J. Unguris, R. J. Celotta, and D. T. Pierce, Phys. Rev. Lett. **67**, 140 (1991).
- ⁸G. Chobrok and M. Hofmann, Phys. Lett. **57A**, 257 (1976).
- ⁹E. Kisker, W. Gudat, and K. Schröder, Solid State Commun. **44**, 591 (1982); J. Unguris, D. T. Pierce, A. Galys, and R. J. Celotta, Phys. Rev. Lett. **49**, 72 (1982); H. Hopster, R. Raue, E. Kisker, G. Güntherodt, and M. Campagna, *ibid.* **50**, 70 (1983).
- ¹⁰R. J. Celotta and D. T. Pierce, in *Microbeam Analysis*, edited by K. F. J. Heinrich (San Francisco Press, San Francisco, 1982), p. 469.
- ¹¹J. Kirschner, Scanning Electron. Microsc. **III**, 1179 (1984).
- ¹²K. Koike and K. Hayakawa, Jpn. J. Appl. Phys., Part 2 **23**, L187 (1984).
- ¹³K. Koike, H. Matsuyama, and K. Hayakawa, Scanning Microsc. Suppl. **1**, 241 (1987).
- ¹⁴R. Allenspach, IBM J. Res. Dev. **44**, 553 (2000).
- ¹⁵G. G. Hembree, J. Unguris, R. J. Celotta, and D. T. Pierce, Scanning Microsc. Suppl. **1**, 229 (1987).
- ¹⁶H. P. Oepen and J. Kirschner, Scanning. Microsc. **5**, 1 (1991).
- ¹⁷D. L. Abraham and H. Hopster, Phys. Rev. Lett. **58**, 1352 (1987).
- ¹⁸T. Kohashi and K. Koike, Jpn. J. Appl. Phys., Part 2 **40**, L1264 (2001).
- ¹⁹H. P. Oepen and H. Hopster, in *Imaging of Magnetic Nanostructures*, edited by H. Hopster and H. P. Oepen (Springer, Berlin, 2002).
- ²⁰J. Kirschner and S. Suga, Solid State Commun. **64**, 997 (1987).
- ²¹G. Steierl, W. Lutzke, H. P. Oepen, S. Tegen, C. M. Schneider, and J. Kirschner, *Proceedings, Magnetoelektronik, Beiträge zum BMBF-Statusseminar Magnetoelektronik, Dresden 2000* (VDI-Technologiezentrum, Düsseldorf, Germany, 2000), p. 341.
- ²²E. E. Huber, Jr., D. O. Smith, and J. B. Goodenough, J. Appl. Phys. **29**, 294 (1958).
- ²³R. M. Moon, J. Appl. Phys. **30**, 82S (1959); S. Methfessel, S. Middelhook, and H. Thomas, *ibid.* **31**, 302S (1960).
- ²⁴G. Steierl, H. P. Oepen, and J. Kirschner (unpublished).
- ²⁵T. VanZandt, R. Browning, and M. Landolt, J. Appl. Phys. **69**, 1564 (1991).
- ²⁶K. J. Kirk, J. N. Chapman, and C. D. W. Wilkinson, Appl. Phys. Lett. **71**, 539 (1997).
- ²⁷A. Hubert and R. Schäfer, *Magnetic Domains: The Analysis of Magnetic Microstructures* (Springer, Berlin, 1998).